2019 International Symposium on Lightning Protection (XV SIPDA), São Paulo, Brazil, 30th September – 4th October 2019.

Experimental Validation of Electrical Model Residual Voltage Test Circuit in Surge Arresters

William Moreira de Assis
High and Extra High Voltage Laboratory of UFPA
Universidade Federal do Pará
Belem, Brazil
Willassis60@gmail.com

Alander Rocha Ribeiro
High and Extra High Voltage Laboratory of UFPA
Universidade Federal do Pará
Belem, Brazil
alanderribeiro1995@gmail.com

André Melo Moraes
High and Extra High Voltage Laboratory of UFPA
Universidade Federal do Pará
Belem, Brazil
Andre_mel_mor@hotmail.com

Antonio Fernando Martins Cardoso
High and Extra High Voltage Laboratory of UFPA
Universidade Federal do Pará
Belem, Brazil
Antoniocardoso1989@gmail.com

Adriane Barbosa de Brito
CELPA
Universidade Federal do Pará
Belem, Brazil
anebarb86@yahoo.com

Mellina Modesto Lisboa
High and Extra High Voltage Laboratory of UFPA
Universidade Federal do Pará
Belem, Brazil
mellinalisboa@gmail.com

Marcus Vinicius Alves Nunes
High and Extra High Voltage Laboratory of UFPA
Universidade Federal do Pará
Belem, Brazil
mvanprof@gmail.com

Allan Rodrigo Arrifano Manito
High and Extra High Voltage Laboratory of UFPA
Universidade Federal do Pará
Belem, Brazil
Allanarrifano@gmail.com

Adonis Ferreira Raiol Leal
LRL - Lightning Research Laboratory
Universidade Federal do Pará
Belem, Brazil
adonisleal1@gmail.com

***Abstract*—This work proposes the adoption of an electric model for residual voltage tests in zinc oxide (ZnO) arresters for standardized and non-standardized waveforms, Lightning current waveform models already consolidated in the literature were used. The proposed model was validated by tests performed at the UFPA High and Extra High Voltage Laboratory (LEAT), n the tests, it was measured residual voltage and discharge current in the arrester. It was applied a discharge current of 10kA in the arrester with nominal voltage of 30kVrms. Additionally, simulations were performed in the ATP Draw software to evaluate the accuracy of the model for waveform 8/20µs. The resultant model was compared to the measurement results. The model proved to be satisfactory for all impulsive waveforms. The parameters of the model are easy to determine, and all necessary information for the lightning arrester and pulse generator is contained in manufacturers' manuals and catalogs.**

Keywords— Electrical model; surge arresters; residual voltage test; current impulses.

I. Introduction

The electrical system, in general, is subject to the incidence of lightning or surges of switching. In order to prevent high-cost equipment from suffering significant damage to their insolation, protective devices such as surge arresters are used, which are most suitable to perform this function [1]. In this context, the surge arresters has a predominant role in the reliability of the electrical systems, since its inoperation would leave the equipment under its protection vulnerable to the surges that can occur in the system. Commonly, they are installed in the input of the substations or at the high voltage terminals of power transformers.

The most used protective equipment is the Metal-Oxide Surge Arresters (MOSA). This is a structure formed by the stacking of non-linear resistors, called varistors, surrounded by a polymeric or porcelain sheath [2]. Its operation is based on the retention of lightning and switching surges, reducing the transient overvoltage amplitudes in the equipment terminals or the protected systems to pre-established levels.

The high-intensity current flowing in the arresters cause an overheating in the MOSA tablets due to avalanche of electrons. This situation became problematic, becouse results in the necessity of a break time between the pulse applications, making it necessary to increase the time of the tests in order to compare with the simulation results.

The residual voltage test indicates the permissible overvoltage levels for the arrester when a nominal discharge current flows through it. This voltage is an important parameter for coordination calculations of insolation of the network.

The tests are performed in high voltage laboratories using a current impulse generator, use arresters that are subjected to standard high-current pulses and the residual voltage values at their terminals are measured [3]. However, the generator configuration and the circuit load voltage level is still empirically adjusted and estimated by the manufacturer's experience, which generates a small discrepancy in the inductance values of the pulse generator when simulations are performed with the same parameters as will be presented in this paper.

Aiming at a better efficiency in testing, it has been proposed a simulator for residual voltage tests in surge arrester in *ATP Draw*, analyzing circuit parameters with the actual test data in the High and Extra High Voltage Laboratory (LEAT). Thus, the modeling is performed using a configuration established by the manufacturer of the pulse generator. Comparisons between the computational model implemented in the ATP and the test carried out at LEAT will be made in order to validate the simulations and verify the influences of the cable inductances.

II. CURRENT IMPULSE GENERATOR

A current impulse generator is an equipment composed of several components such as: impulse capacitors, spark plugs, impulse forming elements, earthing switch and others. It is used to generate pulses of high currents for or performing different tests in surge arresters and varistors. Such pulse is shown in Fig. 1.

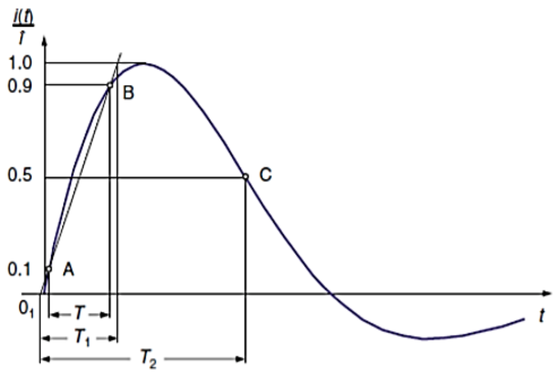

Fig. 1. An example of an exponential impulse current with its tail intersecting the origin.
Source: [4]

According to Fig. 2, a capacitor is charged initially by a source of continuous voltage and discharged to the RL assembly upon key closure of the spark type. The parameters R and L are responsible for by setting the parameters T1 and T2.

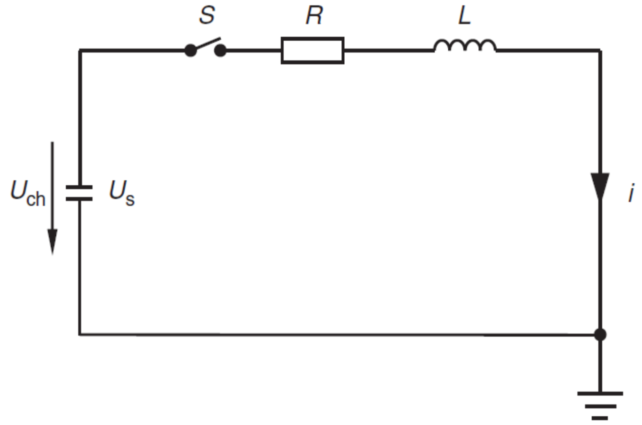

Fig. 2. Simplified model of the current impulse generator.
Source: [4]

B. LEAT-UFPA Current Impulse Generator

The generator used as the basis for modeling in ATP is shown in Fig. 3, and is located in the LEAT-UFPA. It has 12 stages, 1.2MV and 120 kJ powered by a rectifier acting as a high voltage DC source, 12 charging capacitors, 12 inductors (10 inductors of 30μH and 2 inductors of 10μH), load and equipotentiation, a capacitive divider for measuring the resistive shunt for current measurement and one control unit.

Fig. 3. LEAT-UFPA current impulse generator.

C. Computational model of MOSA

The model chosen for the proposed simulations is based on IEEE WG 3.4.11 and is shown in Fig. 4. The inductance L1 is presented between the non-linear resistors A0 and A1, as well as a capacitance C. A resistor R in the order of GΩ is used to avoid numerical oscillations [5]. This model is based on a zinc oxide tablet with nominal voltage of 1 kV, so that there is a residual voltage reference value. Surge arresters with rated voltages greater than 1kV have multiple residual voltages from the residual voltage values for a chip.

The model proposed by Fernandez is shown in Fig. 4.

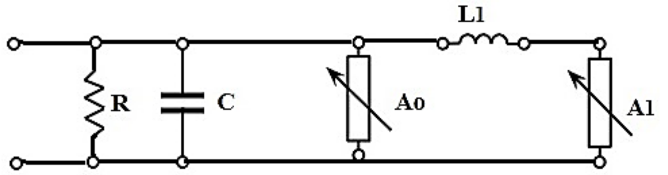

Fig. 4. Model proposed by Fernandez.
Source: [5]

D. Surge arrester data

The surge arrester data and generator configurations used in tests in the LEAT are shown in Table I e II

TABLE I SURGE ARRESTER DATA

Nominal Voltage (kV)	MCOV(kV)	Residual Voltage for 5kA, 8/20μs
30	24,4kV	93kV

TABLE II GENERATOR CONFIGURATION USED

Generator configuration	1s2p (1 series, 2 parallel)
Load Voltage per stage	Approximately: 50kV – 90kV
Current Shunt	SH-Q-0.1 (0,1 Ω)
Internal Series Resistor	No
Internal Inductance:	$30\mu H + 1x10\mu H//30\mu H$

III. SIMULATIONS AND RESULTS

For the simulation of the residual voltage test in the arrester, two pulses were used: one of 5 kA, 50% of the nominal discharge of the arrester, and another of 10 kA, 100% of the nominal discharge of the same arrester. Both pulses have a virtual forward time ($T1$) of approximately 8 μs and a half-time ($T2$) of, approximately, 17 μs, for a pulse polarity inversion not exceeding 20% of the current crest, as recommended by the standards.

In order to generate a more didactic and adequate representation of the equivalent circuit of the LEAT generator, some adaptations were made in the circuit. The result is shown in Fig. 5. The changes made were:

• Preloaded capacitors were used in the simulation, since, basically, the DC source (rectifier) charges them moments before the capacitors are unloaded, thus not influencing the waveform.

• The key simulates the behavior of the generator spark. The switching time of this switch is greater than the time constant of the circuit so as to guarantee the total unloading of the capacitor.

• Removal of the external resistor: The impulse current waveform, obtained in the LEAT current impulse generator, did not show distortion (or damping). So, the external resistance associated with the ohmic losses and the skin effect was neglected, therefore, $R_{ext} = 0$.

• Non-existent internal resistor in the LEAT current impulse generator circuit, it is possible to only make modifications to the internal inductance of the circuit, limiting the generator to only perform discharge current close to the 8/20μs waveform.

• Insertion of the capacitor divider with damping resistor: The task of the voltage divider is to allow the capture of the residual voltage under the test object. In addition, deliver at the terminal output a real small-scale copy of the voltage of the object under test. Another task of the capacitor divider with damping resistor is to reduce the voltage oscillations due to traveling waves. For the simulated circuit, it decreases the oscillation due to the numerical convergence of the ATP. However, due to its low value, it does not interfere in a significant way in the result, only acts on the decrease of the oscillation.

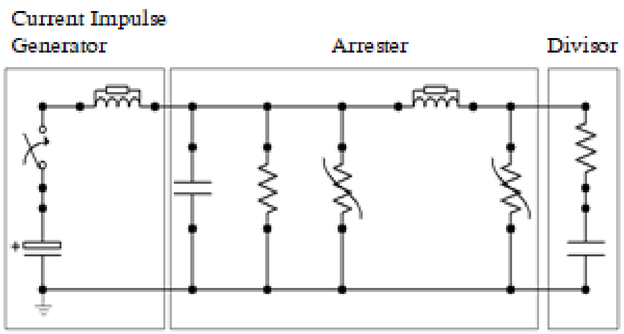

Fig. 5. Impulses generator model, voltage divider and Fernandez's arrester model [5] on ATP.

The waveforms obtained in the ATP simulations are shown in Fig. 6 and 7. The waveforms obtained in the LEAT residual stress tests are shown in Fig. 8 and 9. They come from the Hias 773 data acquisition software from the manufacturer Haefely, through a report tool.

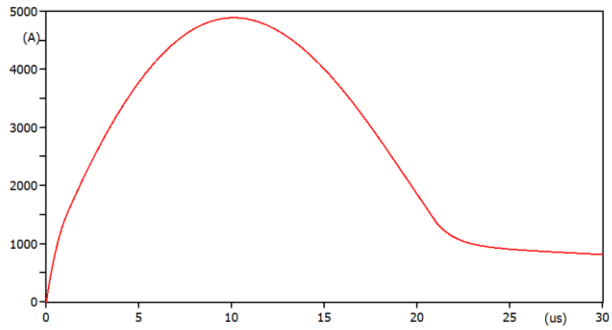

Fig. 6. Discharge current 5kA, arrester of U_n =30kV.

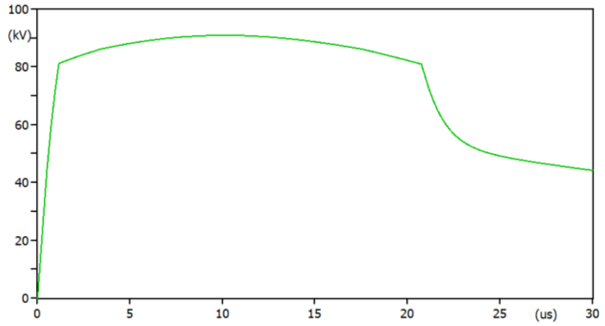

Fig. 7. Residual voltage for discharge current of 5kA, arrester of U_n =30kV.

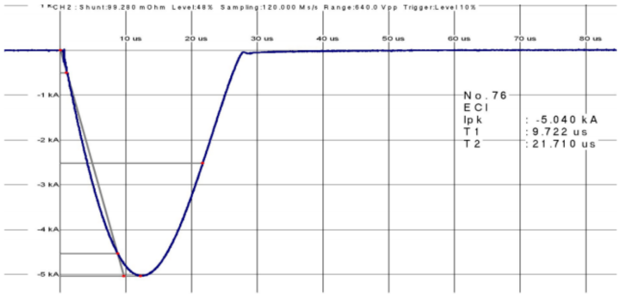

Fig. 8. Discharge current of 5kA waveform on DIAS 773.

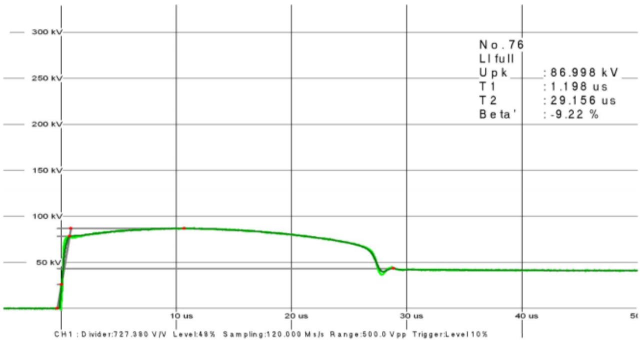

Fig. 9. Residual voltage waveform on DIAS 773.

The waveforms produced in the test and in the simulations showed similarities, with differences in the front and tail times. However, this is due to the modelling of inductance and capacitance parameters of the circuit, where only the capacitances of the charging capacitor and the series inductance of the generator circuit were considered.

Discharge currents with similar values were obtained, and the charge voltage of the capacitors in the simulation were adjusted with the trial and error method. But we note in Table III a difference in values between the residual voltage measured in the test and that found in the simulation, this is due to the actual residual voltage value found of the arrester, since it was acquired with the residual voltage tests for the form of 8/20µs and discharge current amplitude of 10kA.

TABLE III WAVEFFORM PARAMETERS FOR THE RESIDUAL VOLTAGE TEST; COMPARISON OF TEST AND SIMULATION VALUES.

Set up 2 stages, C=1,0µF

ATP simulation			**Current Impulses Generator Tests**		
Discharge current (kA)	**Residual voltage (kV)**	**Waveform (µs)**	**Discharge current (kA)**	**Residual voltage (kV)**	**Waveform (µs)**
4,9	91,05	8,07/18,75	5,040	85,92	9,722/21,710

Thus, the parameter calculations were repeated for the actual residual voltage value of the arrester, and no longer the maximum residual voltage value found in the manufacturer's catalogue, changing all parameters of the model to be simulated in the ATP.

According to [8], the inductance of thin metal strips can be calculated by (1).

$$L = 0{,}002 \times l \left[\ln\left(\frac{4 \times l}{d}\right) - 1.0 + \frac{d}{2 \times l} + \frac{\mu_r T(x)}{4} \right] (\mu H) \quad (1)$$

$$T(x) = \frac{\sqrt{0.873011 + 0.00186128x}}{1 - 0.278381x + 0.127964x^2} \quad (2)$$

$$x = 2\pi r \sqrt{2\mu \frac{f}{\sigma}} \quad (3)$$

Where r is the conductor radius in cm, µ is the absolute magnetic permeability of the conductor and σ is the conductivity of the conductor.

However, it was verified that cable inductances influenced the residual voltage and discharge current waveforms; in which these inductances and capacitances are intrinsic to the physical parts and connections of the generator. To estimate these values, they were calculated according to the equation above taking their physical dimensions into account, and also by means of inductance increments in the simulated circuit to obtain waveforms close to the waveform obtained in the laboratory test.

In Fig. 10, 11 and 12, there are the test circuit and the connections between the generator and the arrester.

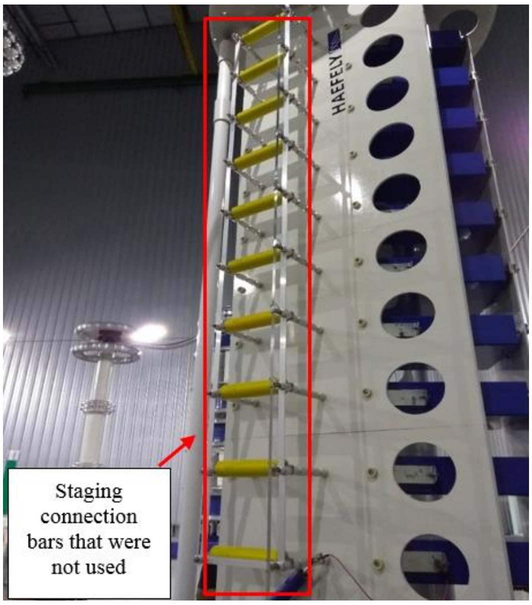

Fig. 10. Short-circuit bars of unused stages in the current pulse generator

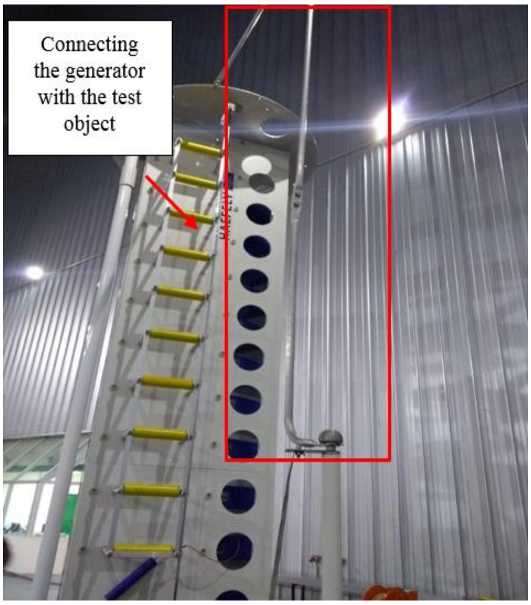

Fig. 11. Connection bars from the last stage of the generator to the insulation support of the test object

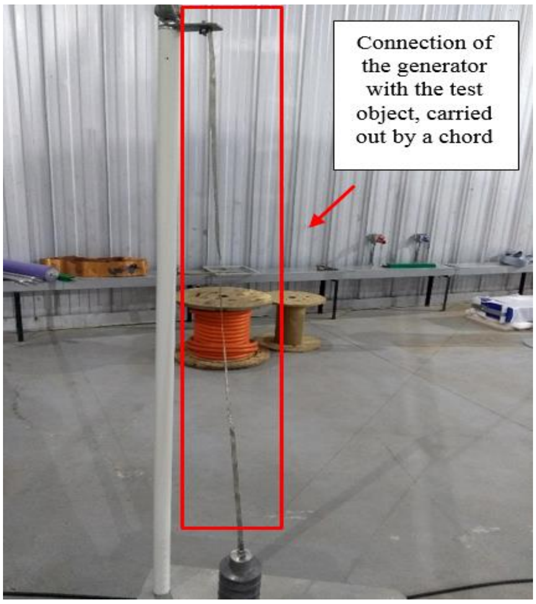

Fig. 12. Aluminum rope for connection to the surge arrester.

Using (1), and considering the crest time of the waveform of 8µs, we have a frequency of 125kHz. For the Aluminium Material, which has relative permeability µr = 1.00002 and conductance σ = 3.72x10-7 S/m, an inductance associated with the circuit connections of L = 12.442µH is obtained.

We can associate the value of the inductance of the connections to the inductance parameter of the generator Lg, and with that, affirm that the total inductance of the circuit is due to the discharge inductance of the generator (a variable parameter of the circuit), added to the intrinsic inductance of the generator with the surge arrester.

Another important point is that the arrester manufacturer data shows the maximum residual voltage values that it can achieve for the purpose of commissioning calculations of the isolation coordination.

Thus, when the laboratory test was carried out, it was noticed that the values of residual voltage in the arrester were lower than the manufacturer data, attesting a good performance of the same in front of the discharge current in the values of 5kA and 10kA.

However, when the parameters of the arrester model were found, it can be seen that the residual voltage peak value arrester. Due to that, an update was made on the residual voltage value of the arrester used, changing the value of manufacturer, 99kV, to the values found in the test, of 94kV.

From these adaptations and corrections, new values can be found for the total inductance parameters of the generator circuit and also the new maximum residual voltage reference for the calculations of A0, A1 and Lpr. Fig. 13 shows the ATP circuit.

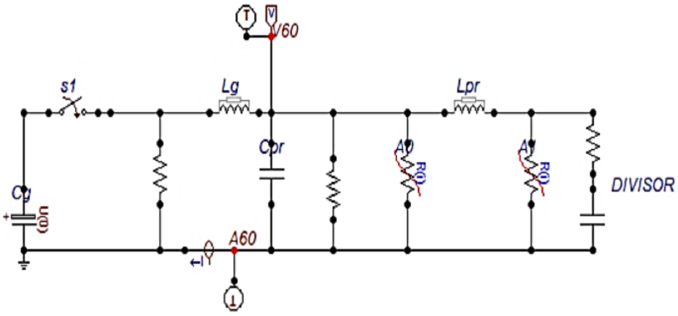

Fig. 13. Test circuit implemented in ATP Draw.

The results obtained are shown in Fig. 14, 15, 16 and 17, and compared in Table IV, where a correspondence between the waveforms obtained in the simulations with the ones obtained through laboratory test can be seen.

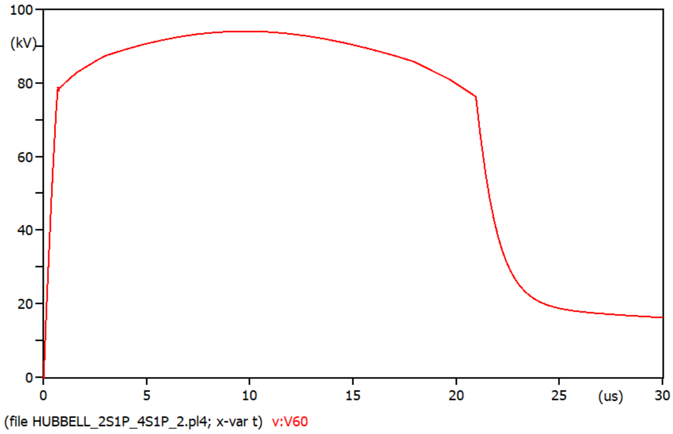

Fig. 14– Residual Voltage for 10kA 8 / 20µs Discharge Current in ATP Draw.

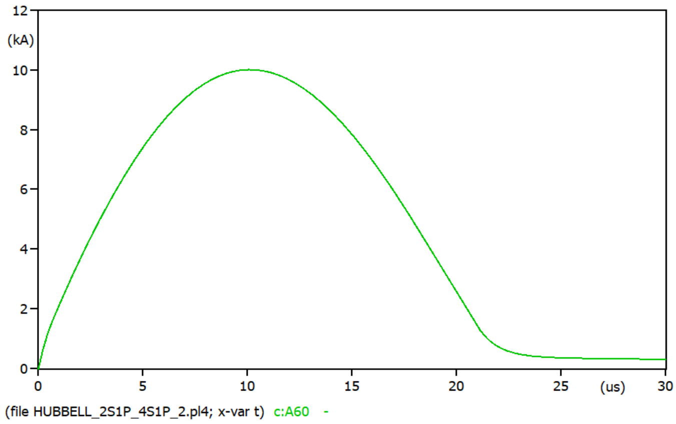

Fig. 15. 10kA 8 / 20µs Discharge Current

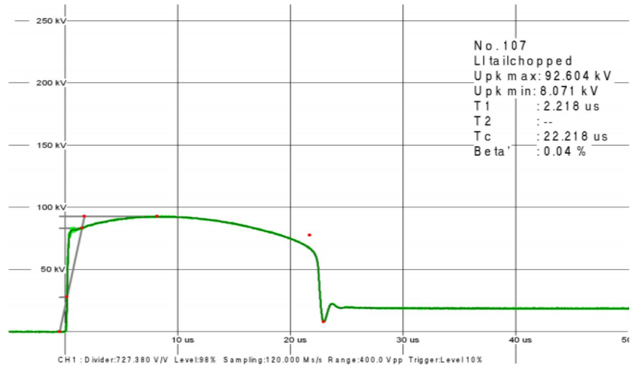

Fig. 16. Residual voltage for discharge current 10kA 8 / 20µs in the laboratory test.

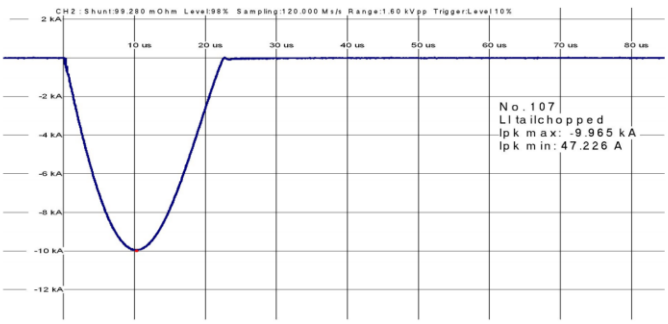

Fig. 17 - Discharge Current 10kA 8 / 20µs.

TABLE IV WAVEFFORM PARAMETERS FOR THE RESIDUAL VOLTAGE TEST; COMPARISON OF TEST AND SIMULATION VALUES.

Set up 2 stages, C=1,0µF

ATP simulation			Current Impulses Generator Tests		
Discharge current (kA)	**Residual voltage (kV)**	**Waveform (µs)**	**Discharge current (kA)**	**Residual voltage (kV)**	**Waveform (µs)**
9,977	93,3	8,14/17,73	9,965	93,2	8,075/17,05

IV. CONCLUSION

In this work, a computational model was proposed to evaluate the residual voltage test on Zinc Oxide arresters. For that, the performance of a surge arrester was evaluated for amplitude values of 5kA and 10kA and different discharge current waveforms. From the results of the tests it was possible to determine the behavior of the RLC circuit of the voltage generator and also the performance of the computational model chosen to represent the operation of the arrester for high currents and high frequencies.

The model of the pulse generator and the arrester were implemented and discharge currents of 5kA and 10kA were applied according to current norms in order to measure their residual voltage both in the laboratory and in the computational environment, obtaining a comparison between the methods.

The responses of the model were initially not satisfactory because, only the external inductance of the generator was taken into account, but it was analysed by comparison that the inductance of the simulated circuit did not correspond to that of the laboratory test. From this it was possible to understand the influence of metallic connections for high frequency signals in the inductance of the circuit and estimate these values of connections, in order to integrate them to the computational model.

Subsequently, satisfactory results were obtained for discharge currents of 5kA and 10kA for standard waveforms of 8/20µs. Thus it was possible to find all possible waveforms for the available inductors in the laboratory and know the limitations of the generator and discover better configurations for tests.

Hence, it is possible to perform preliminary tests computationally through simulations, and so, carry out the least possible current impulse applications that can cause damage to the arrester and consequently decrease the test time in an equipment in the laboratory, since after a discharge application, the specimen has an increase in temperature due to the thermal avalanche of the electrons, and it is necessary to wait a few minutes for the reestablishment of its temperature.

From this study, it is also possible to predict the purchase of peripherals as capacitors, inductors and resistors for better adaptation to a specific test demanded by the research or high voltage tests market.

Based on all these analyses, it can be concluded that the proposed computational model for residual voltage tests is satisfactory. In addition, it makes the execution of laboratory tests much more efficient because the tests are performed previously with the arrester manufacturer data and the best configuration of the current pulse generator.

ACKNOWLEDGMENT

We thank the P&D Program regulated by ANEEL and CELPA, CEMAR and Equatorial that supported the project. And thanks to FAPESPA, who gave financial support and encouragement to this work.

REFERENCES

[1] M. M. Diniz, “Ensaios e avaliação elétrica de um novo projeto de para-raios para sistemas de distribuição em média tensão”, Dissertação de mestrado, UNIFEI, Itajubá, 2011.

[2] E.T. Wanderley Neto, E.G. da Costa, R. T. de Souza, E. C. T. de Macedo, M. J. A . Maia, “Monitoração e Diagnósticos de Para-ráios a ZnO” IEEE Latin America Transection, Vol. 4. No. 3, 2006K.

[3] K.. Schon, “High Impulse Voltage and Current Measurement Techniques”. Braunschweig: Springer, 2013, 272 p..

[4] C.L. Wadwha, “High Voltage Engineering, Second Edition, New Age International Publishers”, New Delhi, 2007.M. Young, The Technical Writer’s Handbook. Mill Valley, CA: University Science, 1989.

[5] R. Diaz, F. Fernandez, J. F. Silva, “Simulation and tests on surge arresters in high-voltage laboratory”. IPST 2001, High-Voltage Laboratory, National University of Tucuman, 4000 Argentina., jun. 2.

[6] ASSOCIAÇÃO BRASILEIRA DE NORMAS E TÉCNICAS, “NBR 16050: Para-raios de resistor não linear de óxido metálico sem centelhadores para circuitos de potência de corrente alternada”. Rio de Janeiro, 2012.

[7] “Manual do Gerador de Impulso de Corrente de 1200 kV/20 kA”, Haefely, Suíça, 2011

[8] C.R. Paul, “Analysis of multiconductor transmission lines”, 2nd ed, 2008.